

Supporting Information

Heating-Rate Controlled Defect Engineering in BiVO₄ Thin Films for Enhanced Photoelectrochemical Water Splitting

Table S1. Summary of recently reported strategies for improving the current density of BiVO₄.

Study / Reference	Synthetic Protocol	BiVO ₄ Type	Current Density (mA/cm ²)	Electrolyte Composition	Key Highlights and Comparative Advantages
Fu et al., <i>Nanomaterials</i> , 2024	Spin Coating + Annealing	Pristine BiVO ₄	2.94	Borate buffer (pH 9.3)	Less control over defect location; requires high-pH buffer; lower photocurrent
Zhang et al., <i>Nat. Commun.</i> , 2024	Surface Dipole Engineering	Pristine BiVO ₄	3.6	KPi (pH 7.0)	Complex surface treatments; less scalable; stability not reported
Liu et al., <i>PCCP</i> , 2023	DFT-Engineered Vacancy Distribution	Pristine BiVO ₄	2.9	KPi + Na ₂ SO ₃ (pH 7.0)	Theoretical focus; lacks experimental validation and stability test
Han et al., <i>EES</i> , 2018	Laser Ablation	Pristine BiVO ₄	3.6	KPi buffer (pH ~7.0)	High photocurrent but uses laser ablation, which is costly and non-scalable
Wu et al., <i>Appl. Catal. B</i> , 2018	Multi-layer Deposition	Pristine BiVO ₄	3.1	KPi + CoPi (pH ~7.2)	Multi-layered process; moderate stability; lower control of morphology and Ov
This Work (2025)	Spin Coating + Controlled Heating Rate	Pristine BiVO ₄	3.17	0.1 M Na ₂ SO ₄ + 0.1 M Na ₂ SO ₃ (pH ~9.26)	Scalable and simple method; optimized heating rate creates Ov without doping or cocatalysts; reduces bandgap to 2.33 eV; superior surface porosity; 4.5 h stability

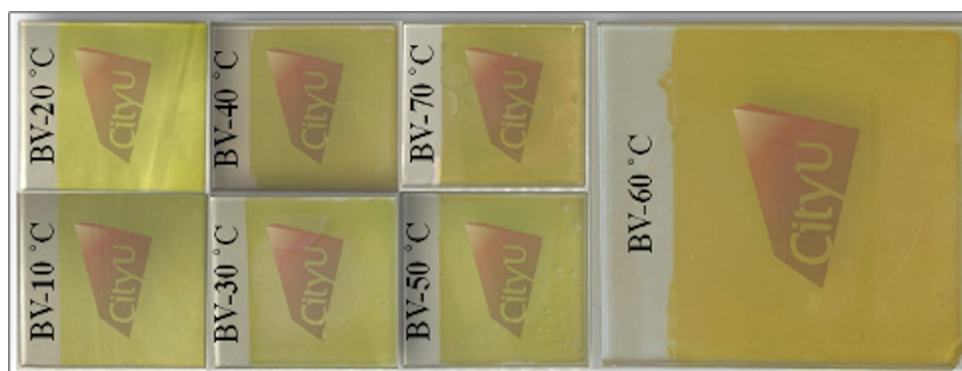


Figure S1. Digital photographs of as prepared samples at selected heating rates.

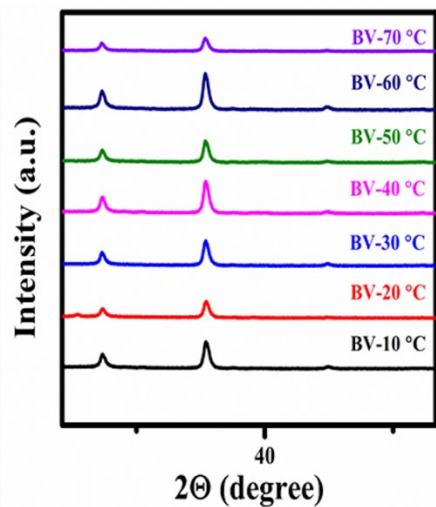


Figure S2. Magnification of XRD peak intensities.

XRD Peaks	Associated planes
18.91	101
28.8	112
30.4	004
37.6	211
42.3	105
46.7	204
53.4	301
54.7	312

Table S3. indicating XRD peaks observed in all samples and their respective planes.

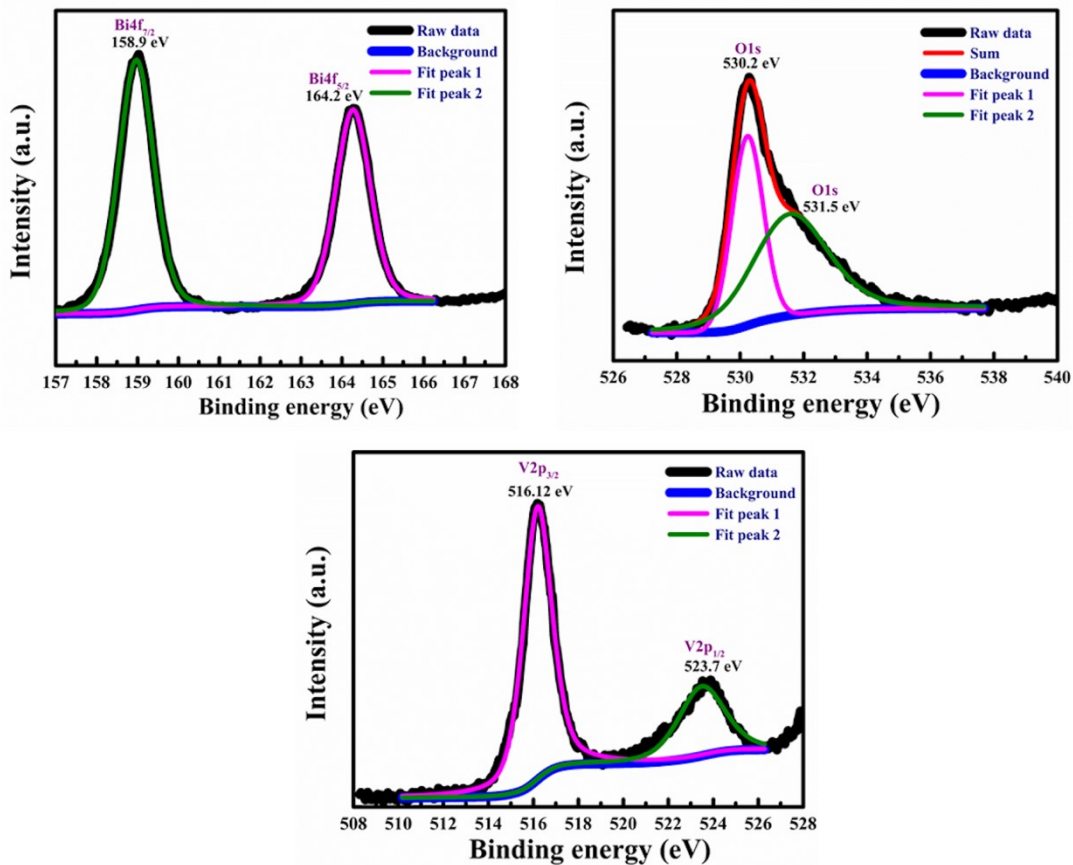


Figure S4. XPS peaks deconvolution for splitting bands of Bi_{4f}, O1s, and V2p (BV-60 °C), an intense peak at 531.5 eV for O1s is indicating the richness of this sample in oxygen vacancies.

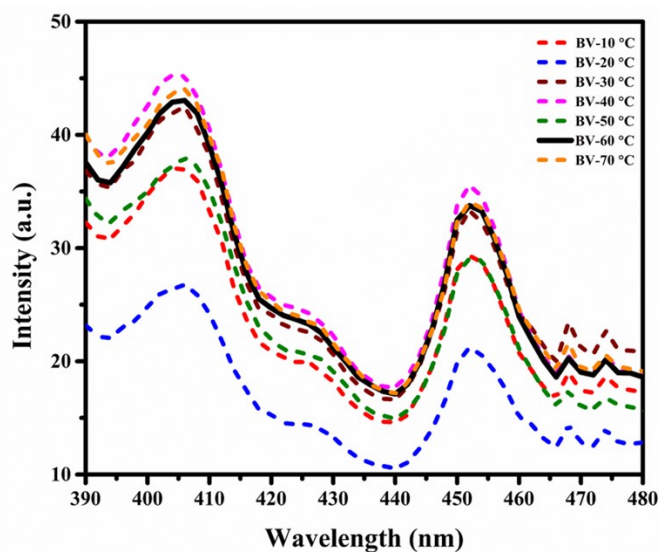


Figure S5. Photoluminescence (PL) spectroscopy of BiVO₄ films annealed at different heating rates.

Supplementary note 1. PL spectroscopy is a data collected by the recombination of photogenerated electrons-hole pairs. Hence if the intensity of the curve obtained is higher, the higher will be the recombination of photogenerated charges. In other words, the material will exhibit lower photoactivity, because most of the charges will recombine beforehand their participation in photocurrent generation. Figure S5 represents the PL spectra of BiVO₄ samples, where BV-60 °C is exhibiting charge recombination as high as BV-30 °C, BV-40 °C, and BV-70 °C. If we see I-t curves (Figure 5a), the photocurrent density of BV-60 °C is the highest among all the samples which tells that its charge generation property is excellent. If a material generates higher number of photoelectrons with a poor charge trapping property, the charge recombination curve (PL) should be as high as I-t curve among all the samples. But, here the PL spectra of BV-60 °C exhibited the charge recombination at the same rate as BV-30 °C, BV-40 °C, and BV-70 °C. Hence, oxygen vacancies rich BV-60 °C suppressed charge recombination process efficiently which resulted in achieving remarkable photocurrent density.

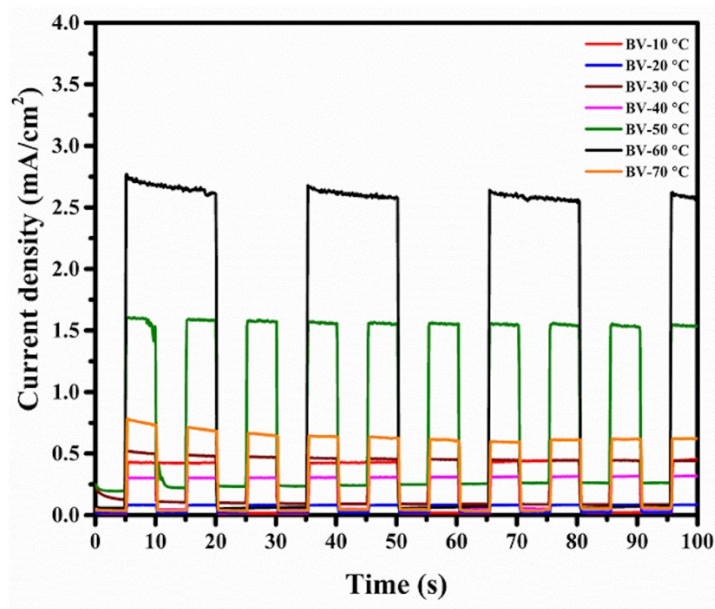


Figure S6. Chopped transient current density under the EE (electrode to electrolyte) illumination at 1.23 V vs. RHE.

References

1. H. Fu, X. Chen, Y. Liu and M. Zhao, *Nanomaterials*, 2024, 14, 1270.
2. L. Zhang, H. Wei, T. Wu and Y. Li, *Nat. Commun.*, 2024, 15, 1–11.
3. Y. Liu, Z. Chen, J. Zhao and Y. Wang, *Phys. Chem. Chem. Phys.*, 2023, 25, 19324–19332.
4. H. S. Han, S. Shin, H. H. Lee and J. H. Kim, *Energy Environ. Sci.*, 2018, 11, 1299–1306.
5. J. M. Wu, L. Zhang, D. Chen and X. Jiao, *Appl. Catal. B: Environ.*, 2018, 221, 187–195.